13th Australasian Fluid Mechanics Conference
Monash University, Melbourne, Australia
13-18 December 1998

LOW-DIMENSIONAL MODEL OF A PLANE TURBULENT MIXING LAYER

Laurent CORDIER[(1)], Christian TENAUD[(2)] and Joël DELVILLE[(1)]

[(1)] L.E.A. - UMR CNRS 6609 – 43, Route de l'Aérodrome, 86036 POITIERS CEDEX, FRANCE
[(2)] L.I.M.S.I. - UPR CNRS 3251 – B.P. 133, 91403 ORSAY CEDEX, FRANCE

ABSTRACT

A snapshot-POD is derived from a Large Eddy Simulation (LES) of a plane turbulent Mixing Layer (ML). The obtained eigenfunctions are found in good agreement with experiments. Finally a Low-Order Dynamical System (LODS) is derived. The random coefficients obtained from the LODS and the ones directly calculated from the LES are compared.

INTRODUCTION

The active control of fully developed turbulent flows is of particular interest for many industrial applications. In shear flows, large-scale Coherent Structures (CS) exist which contain most of the turbulent kinetic energy. These CS are mainly responsible for vibrations, noise generation, etc. Therefore, in term of control, it seems important to describe correctly the characteristics of these CS and to predict their time evolution using models as simple as possible. One method proposed to mimic the dynamical behavior of the flow is to develop a LODS. In the Proper Orthogonal Decomposition (POD) (Lumley 1967), the CS are defined in terms of optimal signature of the turbulent kinetic energy. The CS are then related to the eigenfunctions of the POD. From these eigenfunctions, a LODS can be derived through a Galerkin procedure. This method was, for example, successfully used to study the near-wall evolution of the flow within a turbulent boundary layer (Aubry *et al.* 1988).

The aim of the present study is to apply such procedures on the data from the LES of a 3D ML spatially developing downstream of a flat plate. The LES has been performed on a well documented flow configuration studied experimentally in details in earlier works (Delville 1994, 1998, Cordier *et al.* 1997, Bonnet et al. 1998). Several gains can be derived from such a LES. Mainly the whole flow field is known in a deterministic way, thus the efficiency of the POD can be analyzed and the time evolution of the POD modes studied in details. The data-base generated by the LES can be used to check assumptions that are required when experimental procedures are applied.

THE SNAPSHOT-POD METHOD

In order to analyze the organization present in the flow, the Snapshot-POD method (Sirovich 1987) is applied on the results given from the LES. This POD, based on spatial averaged quantities, has been preferred to the "standard" approach (Lumley 1967). Every spatio-temporal event $v_i(\underline{x},t)$ is decomposed using a mean and a fluctuating part:

$$v_i(\underline{x},t) = \overline{v_i}(\underline{x}) + v_i'(\underline{x},t)\ , \qquad (1)$$

where the mean part corresponds to a time average:

$$\overline{v_i}(\underline{x}) = \frac{1}{T}\int_T v_i(\underline{x},t)\,dt\ .$$

Fluctuating parts are written using a discrete basis:

$$v_i'(\underline{x},t) = \sum_{n=1}^{N^*} A^{(n)}(t)\ \Phi_i^{(n)}(\underline{x})\ , \qquad (2)$$

where N^* is the number of modes solved in the snapshot-POD. $A^{(n)}(t)$ correspond to the eigenfunctions of a Fredholm integral problem:

$$\int_T C(t,t')\ A^{(n)}(t')\,dt' = \Lambda^{(n)}\ A^{(n)}(t)\ , \qquad (3)$$

where $C(t,t')$ is the temporal velocity-correlations:

$$C(t,t') \quad = \quad \frac{1}{T}\int_{\mathcal{D}} v_i'(\underline{x},t)\ v_i'(\underline{x},t')\,d\underline{x} \qquad (4)$$

and where $\Lambda^{(n)}$ are the real, positive eigenvalues of this tensor. Each eigenvalue is associated to the energy density contained in the corresponding mode and the sum of $\Lambda^{(n)}$ is equal to the turbulent kinetic energy included in the integral domain ($\mathcal{D}$). The spatial eigenfunctions are deduced from:

$$\Phi_i^{(n)}(\underline{x}) = \frac{1}{T\Lambda^{(n)}}\int_T v_i(\underline{x},t)\ A^{(n)}(t)\,dt\ . \qquad (5)$$

LARGE EDDY SIMULATION

Details on the LES code can be found in several places, mainly in Lardat *et al.* (1997) or in Ta Phuoc (1994), and are not discussed here.

The LES of the spatial development of the ML starts at the trailing edge of the splitting flat plate. In the simulated flow, the velocity ratio is $r=U_2/U_1=0.59$, where U_1 and U_2 are the magnitudes of the external velocities of the boundary layers at the trailing

edge of the flat plate. The Reynolds number, based on δ_{ω_0} and on $\Delta U = U_1 - U_2$, is 35000 (δ_{ω_0} refers to the vorticity thickness at the exit of the computational domain). The computational domain spreads over 20 δ_{ω_0} in the streamwise direction, 6 δ_{ω_0} in the inhomogeneous (vertical) direction (y) and lays over 5 δ_{ω_0} in the spanwise direction(z), for which the flow is supposed to be periodic.

The grid uses $401 \times 71 \times 55$ nodes in the $x \times y \times z$ directions and is tightened around the centerline of the ML in the direction (y). The grid filter width ($\overline{\Delta} = (\Delta x \times \Delta y \times \Delta z)^{1/3}$) is close to the Taylor micro-scale measured by Delville (1995).

As regards the boundary conditions at the inflow surface (ie. the trailing edge of the splitting plate), the longitudinal component of the mean velocity is initialized using two turbulent Whitfield profiles for the boundary layers from each side of the flat plate. The profiles of the spanwise components of the mean vorticity (Ω_z) are then deduced from the velocity profiles. A white noise is superimposed on Ω_z. The perturbation magnitude is equivalent to an amplitude of $10^{-3}\ U_1$ on the streamwise velocity component. At the outlet boundary ($x = 20\delta_{\omega_0}$), the tangential components of the vorticity (Ω_y and Ω_z) are calculated by extrapolation along the characteristics. The longitudinal velocity component is then deduced from the vorticity profiles, prescribing that the mass conservation is satisfied. At the upper and lower surfaces of the domain ($y = \pm 3\delta_{\omega_0}$), slip conditions are imposed.

VALIDATIONS OF THE SIMULATION

To compare the numerical results with the experimental data, 4000 time steps and a portion of the computational domain ($X/\delta_{\omega_0} \in [5, 15]$) are retained.

Simulated mean velocity and Reynolds stress profiles have been compared with the experimental data (Lardat *et al.*, 1997). The self-similarity behavior of the ML is recovered by the LES ; the spatial growth rate of the mixing layer is correctly predicted (LES: $d\delta_\omega/dx = 0.042$; Exp.: $d\delta_\omega/dx = 0.041 \simeq 0.16\frac{1-r}{1+r}$). Note that this spreading rate is in very good agreement with the Abramovich (1963) rule. Very good agreements are also achieved on the Reynolds stress component.

The agreement between the computations and experiments can also be seen on Fig. 1, where the two-point space correlations $R_{ii}(x_0, y_0, x', y')$ are compared to the space-time correlations measured by Delville (1995). On these figures, the reference point (x_0, y_0) is located at the center of the selected spatial domain. This comparison cross-validates computations as well as experiments. Note that the u component can be described by fluctuations of opposite sign from part to part of the ML, while the v component can be described by fluctuations in phase all over the y direction, alternated in sign in the x direction. Moreover, the shape of the w component indicates the presence of a strong organization for the streamwise vorticity component, this organization being recovered from both experiments and LES.

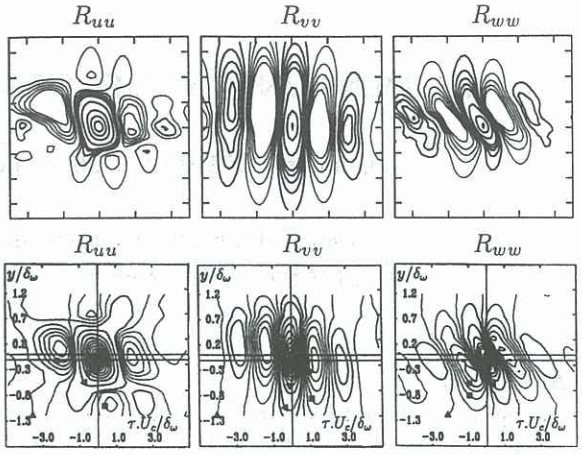

Figure 1: Comparison of the measured space time correlations $R_{ii}(\tau; y, y')$ (bottom) with the space correlations obtained from the LES (top)

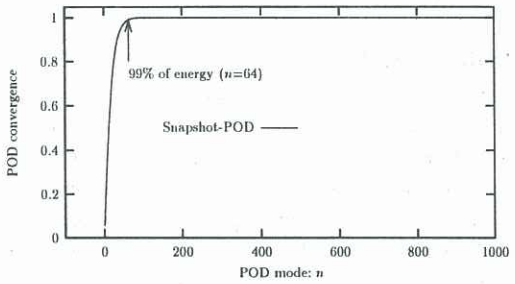

Figure 2: Energy contained in the first 1000 modes of the snapshot POD.

APPLICATION OF THE SNAPSHOT-POD

The convergence of the snapshot-POD, applied on the simulated velocity field, is plotted on Fig. 2. It is found to be very rapid since 99 % of the turbulent kinetic energy is contained within the N_{KL}=64 first modes (generally defined as the Karhunen-Loeve dimension). The relative number of modes required to contain 99% of energy is (N_{KL}/N^*=0.016)

These eigenvalues occur in pair of almost equal values, whereas there is a gap in magnitude between these pairs. The eigenvalue problem (3) is near degenerated. To understand the consequence of this result we present in Fig. 3 positive iso-surfaces of $\Phi_i^{(n)}(x, y, z)$ for the first two modes. Several general features can be noticed when considering these eigenfunctions. Whatever the velocity components are, one can notice a streamwise shift when comparing modes 1 and 2. It can be seen that, essentially, the eigenfunctions of this pair are representing the

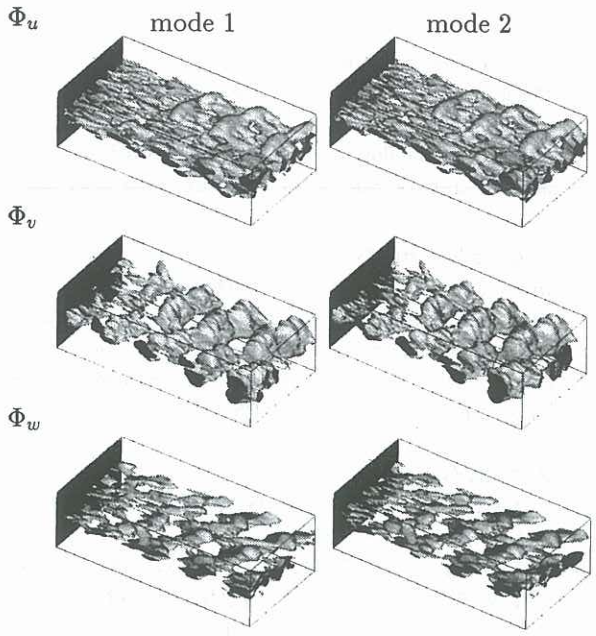

Figure 3: Iso-surface of the spatial eigenfunctions for modes 1 and 2 .

same structure, one of them just being shifted with respect to the other in the streamwise direction. An analogous behavior is observed for the first higher modes. Moreover, these eigenfunctions exhibit a preferred organization in the spanwise direction. Particularly, $\Phi_v^{(n)}(\underline{x})$ is clearly aligned in the spanwise direction and $\Phi_w^{(n)}(\underline{x})$ exhibits lambda-shape like structures (Fig. 3). These behaviors are similar to those observed experimentally by Delville (1994).

LOW-ORDER DYNAMICAL SYSTEM

The goal sought after, is to study the temporal behavior of the large scale coherent structures. Therefore, the temporal approach followed previously by Aubry *et al.* (1988) and Glauser *et al.* (1989) has been employed.

Low-dimensional model: POD-Galerkin procedure

As the pressure field is provided by the numerical simulations, a low-order dynamical system is developed by considering the Navier-Stokes equations written in pressure-velocity formulation:

$$\begin{aligned} \nabla \cdot \underline{\mathbf{V}} &= 0 \\ \frac{\partial \underline{\mathbf{V}}}{\partial t} + \underline{\mathbf{V}}.\nabla\underline{\mathbf{V}} &= -\nabla P + \frac{1}{Re}\Delta\underline{\mathbf{V}} \,. \end{aligned} \tag{6}$$

The velocity ($\underline{\mathbf{V}}$) and the pressure (P) are decomposed using the Reynolds decomposition (1). The velocity fluctuating part is then written using a discrete basis of the flow following equation (2). This decomposition is introduced in the transport equations (6) which are then projected onto the spatial eigenfunctions $\Phi^{(n)}(\underline{x})$ by means of a Galerkin projection. Since the eigenfunctions are orthogonal, a set of N_G time dependent ODEs is obtained for the so-called random coefficients $A^{(n)}(t)$ of the POD:

$$\begin{aligned} \frac{d}{dt}A^{(n)} &= \sum_{m=1}^{N_G} b_{nm}A^{(m)} + P^{(n)} \\ &+ \sum_{m=1}^{N_G}\sum_{k=1}^{N_G} c_{nmk}\left[A^{(m)}A^{(k)} - \overline{A^{(m)}A^{(k)}}\right] , \end{aligned} \tag{7}$$

where N_G is the number of Galerkin modes retained in the dynamical system. The coefficients of the system (7) b_{nm}, c_{nmk} are expressed as follows:

$$b_{nm} = \left(\underline{\Phi}^{(n)}, \frac{1}{Re}\Delta\underline{\Phi}^{(m)} - \nabla\overline{\underline{\mathbf{V}}}.\underline{\Phi}^{(m)} - \nabla\underline{\Phi}^{(m)}.\overline{\underline{\mathbf{V}}}\right)$$

$$c_{nmk} = -\left(\underline{\Phi}^{(n)}, \nabla\underline{\Phi}^{(m)}.\underline{\Phi}^{(k)}\right) \quad \text{and}$$

$$P^{(n)} = -\left(\underline{\Phi}^{(n)}, \nabla P'\right) = -\int_{\partial\mathcal{D}} P'\left(\underline{\Phi}^{(n)}, \underline{n}\right) dS$$

where $\underline{n}$ is the external normal.

These ODEs system is solved using a 4th order Runge-Kutta integration. At the initial state, the random coefficients ($A^{(n)}(t=0)$) are initialized using the projection of the events $v_i(\underline{x},t)$ at $t=0$ on the spatial eigenfunctions. We prescribe $\overline{A^{(m)}A^{(k)}} = \Lambda^{(m)}\,\delta_{mk}$. The b_{nm} coefficients are estimated using the mean velocity given from the LES. The pressure term contribution is neglected in a fashion comparable to Rajaee *et al.* (1994).

Temporal evolution of $A^{(n)}(t)$

The dynamical system was developed on the same record than the previous results. Two sets of Galerkin modes (N_G=10 and N_G = 36) are retained to derive two independent dynamical systems. For these numbers of mode, the relative energy contained in the system is respectively 42% and 90%. The comparisons between the random coefficients $A^{(n)}(t)$, obtained from the resolution of (7), and the projection of the events $v_i(\underline{x},t)$ onto the spatial eigenfunctions $\Phi^{(n)}(\underline{x})$ are plotted for the first two modes on Fig. 4. When considering the early evolution of $A^{(1)}(t)$ ($t < 250$) both dynamical systems are able to follow the temporal evolution of this mode. The same result has been globally observed for higher modes. However, if for a short time integration, a rather good agreement is achieved, it appears that for longer time, the random coefficients $A^{(n)}(t)$ obtained from the dynamical systems diverge from the direct POD projection. For a small truncation (N_G=10), a progressive time shift can be observed. When higher POD modes are included, this time shift can be reduced and the typical period of the modes becomes

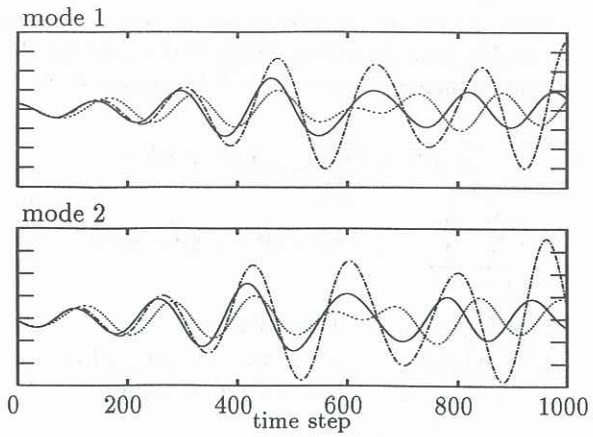

Figure 4: Comparison of the temporal evolution of the first two modes for the snapshot POD —— and the LODS for N_G=10 – – and N_G=36 - - -.

better estimated. Nevertheless, this improvement is associated with a divergence in the amplitude of the first mode. This behavior can be explained by some of the following points. As regards the dynamical system formulation, neglecting the pressure contribution, surely induces some inaccuracy in the model. In the same way, the instantaneous contribution of the averaged field to the dynamical system has been simplified by considering only its temporal average contribution ($\overline{A^{(m)}A^{(k)}} = \Lambda^{(m)}\delta_{mk}$). One last reason for the long term discrepancy can be related to the truncation done in the Galerkin projection. By taking into account additional modes (from N_G=10 to 36), still "energetic" modes have been added, and the system becomes relatively less dissipative. For the dynamical system (N_G=36), tests performed with additional viscosity have shown that the time-shift remains reduced, while the magnitudes of the A coefficients can be lowered.

CONCLUSIONS

A 3D LES of the plane mixing layer have been conducted, from which the history of the 3 velocity components has been calculated on a large temporal sample. From the data base generated by this simulation, a 3 dimensional snapshot-POD has been performed. The spatial organization of the eigenfunctions $\Phi_i^{(n)}$ can be favorably compared to the experimental ones. Finally, the ability of the POD to obtain a low-order dynamical system has been underlined. Two different dynamical systems have been performed using respectively 10 POD modes and 36 POD modes. For short time evolution, the random coefficients calculated from the dynamical systems well agree with the spatial eigenfunctions estimated from the LES results. However, for N_G=36, the dynamical system are not enough dissipative. Artificial dissipation is then necessary to follow correctly the long term temporal evolution of the plane mixing layer.
These first results are very encouraging. In the near future, the influence of adding higher-order POD modes on the flow structure representation will be studied and the role of the pressure term clarified.

Acknowledgments : The LES numerical code was written by Dr Lardat. The authors greatly acknowledge Drs Lardat and Ta Phuoc for their numerous and valuable comments and discussions on the numerics. The calculations have been performed on the Cray C90 of the IDRIS/CNRS Orsay, France.

REFERENCES

ABRAMOVICH,G.N. (1963) *The theory of turbulent jets* MIT Press.

AUBRY, N., HOLMES, P., LUMLEY, J.L. and STONES, E. (1988) *J. Fluid Mech.*, **192**, 115–173.

BONNET, J.P., DELVILLE, J., GLAUSER,M., ANTONIA,R.A., BISSET,D.K., COLE,D.R., FIEDLER,H.E., GAREM, J.H., HILBERG,D., JEONG,J., KEVLAHAN, N.K.R., UKEILEY, L.S.and VINCENDEAU,E. (1998) "Collaborative testing of eddy structure identification methods in free turbulent shear flows". to appear in Exp. in Fluids

CORDIER, L., MANCEAU R., DELVILLE, J. and BONNET, J.-P. (1997) *C. R. Acad. Sci. Paris*, **t. 324**, Série II *b.* 551-557

DELVILLE, J. (1994) *Appl. Scient. Res.* **53**, 263-281.

DELVILLE, J., GAREM H. and BONNET J.P. (1998) in AGARD-AR345 pp. 139-140- April 1998

GLAUSER, M.N., ZHENG, X. and DOERING, C.R. (1989) in *Turbulence and Coherent Structures*, (eds. O. Metais and M. Lesieur), Kluwer Academic Publishers, p. 253.

LARDAT R., BERTAGNOLIO F. and DAUBE O (1997) *C. R. Acad. Sci. Paris*, **t. 324**, Série II*b.*

LARDAT, R., DULIEU, A., SHEN, W.Z., TA PHUOC, L., TENAUD, C., CORDIER, L. and DELVILLE, J. (1997) *Proc. of the IUTAM Symp. on Simulation and Identification of Organized Structures in Flows*, Lyngby, Denmark.

LUMLEY, J.L. (1967) in *Atmospheric Turbulence and Radio Wave Propagation*, A.M. Yagom and V.I. Tatarski, 166–178, Moskow:Nauka.

RAJAEE, M., KARLSSON, S.K.F. and SIROVICH, L. (1994) *J. Fluid Mech.*, **258**, 1–29.

REMPFER, D. (1993) *Phys. Fluids* **6**, (3), 1402–1404

SIROVICH, L. (1987) *Quart. of Appl. Maths.*, **XLV**, N^0 3, 561–590.

TA PHUOC, L. (1994) in *Journée thématique DRET: Aérodynamique instationnaire turbulente - Aspects numériques et expérimentaux.* (eds. DGA/DRET)